Mechanical Resistance of Hot-Mix Asphalt Using Phosphorite as Filler

Hugo Alexander Rondón-Quintana, Ph.D.[1]; Juan Carlos Ruge-Cárdenas, Ph.D.[2]; Fredy Alberto Reyes-Lizcano, Ph.D.[3]; Juan Gabriel Bastidas-Martínez, Ph.D.[4]; and Carlos Alfonso Zafra-Mejía, Ph.D.[5]

Abstract: Phosphorites (PF) have small particle sizes and interesting chemical compositions to be used as filler in asphalt mixtures. The present study assessed the performance that a hot-mix asphalt (HMA) displays when the natural filler (NF) is completely replaced by PF. X-ray diffractometry (XRD), X-ray fluorescence (XRF), and scanning electron microscope (SEM) tests were carried out on NF and PF particles. Asphalt mastic was manufactured using a weight ratio of filler (NF and PF) to asphalt binder of 1:1.2. Penetration, softening point, viscosity, and linear amplitude sweep test were performed on the asphalt mastic. The following tests were carried out on mixes manufactured with NF (control) and PF (HMA-PF): Marshall, indirect tensile strength, Cantabro, resilient modulus, permanent deformation, and fatigue under stress-controlled mode. Additionally, moisture damage resistance was assessed through the tensile strength ratio (TSR) parameter. The HMA-PF mix displayed a better performance in all the evaluated properties, without increasing the optimum asphalt binder content. PF as fillers could be an interesting alternative in the manufacture of HMA mixtures subjected to high temperature climates.
DOI: 10.1061/JMCEE7.MTENG-15720.

Author keywords: Asphalt; Phosphorite (PF); Phosphate rock; Hot-mix asphalt (HMA); Filler.

Introduction

Mineral fillers play an important role in the performance of hot-mix asphalts (HMA) because they make up an important part of the mastic. This material affects the behavior of asphalt mastic and asphalt mixtures (Cheng et al. 2016; Bastidas-Martínez et al. 2021). Different fillers have been studied in HMAs, some more promising than others. Different from the natural ones, the most studied have been hydrated lime, portland cement, fly ash, and slags. Some are used for their good compatibility with asphalt, others for their lower cost, and others for environmental reasons.

In the present study, phosphorite (phosphate rock) was used as a filler. Colombia has important deposits of phosphate rock from sedimentary deposits of marine origin in Huila, Boyacá, and Santander (approximate estimate of availability for exploitation of 370 million tons) (Calle 2016). The production of phosphate rock in Colombia for the year 2016 was 66,324 t (country with sixth highest production in Latin America) (Rojas 2022). It is worth mentioning that in the reviewed literature, no studies were found using phosphate rock as filler in asphalt mixtures. It is generally used as a soil fertilizer. This material was chosen because it shows small particles an interesting chemical composition [comprised mainly of calcium oxide (CaO), phosphorous (P_2O_5), and silica (SiO_2)]. CaO is alkaline and can help increase adhesion with asphalt, and SiO_2 has high hardness and mechanical resistance (Pasandín and Pérez 2015; Rondón-Quintana et al. 2018, 2019, 2020; Sobhi et al. 2020).

Regarding phosphorus, its influence on asphalt is unclear. However, the reference literature shows a material containing phosphorus that had a positive effect on the performance of asphalt binders and asphalt mixtures: polyphosphoric acid (PPA). PPA is a liquid mineral polymer mainly comprised of phosphorus pentoxide (P_2O_5) and phosphoric acid (H_3PO_4) (generally, $P_2O_5/H_3PO_4 > 68\%$). It is a very weak acid in bitumen and it is a cheaper asphalt binder modifier compared with many polymer modifiers (Masson 2008). This chemical modifier was patented in 1973 (Orange et al. 2004; Liu et al. 2018). According to literature, PPA mainly increases high-temperature performance of asphalt binders (increasing its elasticity, stiffness, and rutting resistance) (Aflaki and Tabatabaee 2009; Liang et al. 2017; Jafari et al. 2017; Ge et al. 2017; Hao et al. 2019; Liu et al. 2020; Ma et al. 2021; Song et al. 2021).

The literature is not clear about its effect at low temperatures. Some studies mentioned that PPA has little effect on strength at low temperatures (e.g., Orange et al. 2004; Jafari and Babazadeh 2016; Hossain et al. 2020), whereas others conclude that PPA could weaken the asphalt binder against cracking (Aflaki and Tabatabaee 2009; Liu et al. 2016; Hajikarimi et al. 2018), especially in high concentrations (Ziari et al. 2021). PPA also could improve storage stability of asphalt binders modified with polymers

[1]Full Professor, Facultad del Medio Ambiente y Recursos Naturales, Universidad Distrital Francisco José de Caldas, Carrera 5 Este No. 15-82, Bogotá, DC 110131, Colombia (corresponding author). ORCID: https://orcid.org/0000-0003-2946-9411. Email: harondonq@udistrital.edu.co; harondon2012@hotmail.com

[2]Associate Professor, Civil Engineering Program, Faculty of Engineering, Universidad Militar Nueva Granada, Carrera 11 No. 101-80, Bogotá, DC 111071, Colombia. Email: juan.ruge@unimilitar.edu.co

[3]Full Professor, Dept. of Civil Engineering, Faculty of Engineering, Pontificia Universidad Javeriana, Carrera 7 No. 40-62, Bogotá, DC 110231, Colombia. Email: fredy.reyes@javeriana.edu.co

[4]Associate Professor, Civil Engineering Program, Faculty of Engineering, Universidad Piloto de Colombia, Carrera 9 No. 45A-44, Bogotá, DC 110231, Colombia. Email: juan-bastidas@unipiloto.edu.co

[5]Full Professor, Facultad del Medio Ambiente y Recursos Naturales, Universidad Distrital Francisco José de Caldas, Carrera 5 Este No. 15-82, Bogotá, DC 110131, Colombia. Email: czafra@udistrital.edu.co

Note. This manuscript was submitted on September 29, 2022; approved on January 30, 2023; published online on June 17, 2023. Discussion period open until November 17, 2023; separate discussions must be submitted for individual papers. This paper is part of the ***Journal of Materials in Civil Engineering***, © ASCE, ISSN 0899-1561.

(Qian et al. 2019a; Jiang et al. 2019), and furthermore, it shows good compatibility with asphalt binders (Liu et al. 2018; Qian et al. 2019a). Despite the large number of studies conducted with PPA, the exact reaction mechanism with asphalt binders is not yet fully understood (Masson 2008; Miknis and Thomas 2008; Huang et al. 2011; Liang et al. 2017). However, chemically, PPA increases the amount of asphaltenes, converting aromatics into resins and resins into asphaltenes (Ghabchi et al. 2021).

Other materials with names similar to phosphorite that appear in scientific databases are phosphorous slags (PS) (by-product of the production process of yellow phosphorous) and phosphogypsum slag (PG) (by-product of the production of phosphoric acid). In the field of construction materials, PS has been used mainly to enhance strength, workability, and durability of cement and cement concrete. Additionally, it has been used as a modifier for asphalt binders (Sheng et al. 2017; Qian et al. 2018, 2019b; Yu et al. 2020a, b) and as a replacement of mineral filler in asphalt mixtures (Qian et al. 2013).

PG has been less studied. This material could be used in highway construction. For example, it could replace coarse aggregates in asphalt mixtures (Foxworthy et al. 1996; Katamine 2000) or be used as a modifier for asphalt binders (Cuadri et al. 2014) or as an additive for foamed bitumen (Cuadri et al. 2021). PS and PG showed promising results in studies. However, both contain very low amounts of phosphorus (<2% approximately) in their chemical composition (Cuadri et al. 2014; Maghsoodloorad et al. 2018), and for this reason, they will not be used for analysis or comparison in this study.

The study's main objective was to evaluate the mechanical performance of an HMA mixture when the natural mineral filler (NF) is replaced by phosphorite. The NF used is a limestone-type mineral aggregate. NF was comprised of particles with a size smaller than 0.075 mm (passing through sieve No. 200). In order to evaluate performance, mechanical resistance tests were carried out under monotonic [Marshall and indirect tensile strength (ITS) under dry and wet conditions] and cyclic load (resilient modulus, permanent deformation, and fatigue). Likewise, Cantabro tests were performed to measure abrasion wear resistance. Tests were not carried out to measure properties at low service temperatures because Colombia is a tropical country. On the results obtained, an ANOVA variance analysis was conducted with a reliability level of 95%.

Materials and Methods

Materials

Phosphorite (PF) 28P was used as filler. The manufacturer provides this material in 50 kg laminated polypropylene bags with a maximum moisture of 5%. It is a soil fertilizer made from ground phosphate rock (natural calcium phosphate). It comes from the Media Luna mine located in Aipe (Huila, Colombia). Its particle-size distribution is given in Table 1. PF contains particles with sizes less than 0.85 mm. Specific gravity and absorption [AASHTO T 133 (AASHTO 2019)] of PF is 2.87% and 2.4%, respectively.

Table 1. Particle-size distribution of PF

Sieve	Passing (%)
No. 20	100
No. 40	72.6
No. 80	38.3
No. 200	20.7

The size of the NF (limestone) particles was smaller than 0.075 mm. Specific gravity and absorption of NF is 2.626% and 1.56%, respectively.

Screening tests based on X-ray diffractometry (XRD) and X-ray fluorescence (XRF) were performed on the NF and PF (passing through sieve No. 200) to analyze their mineralogical and chemical composition. XRD samples were poured on an aluminum sample holder, creating the flat surface on which the analysis was carried out. XRF samples were dried at 105°C for a period of 12 h. Samples were molten into pearls subjected to a temperature of 1,000°C, using a borate fusion in a proportion of 1/10. A mixture of lithium metaborate and lithium tetraborate was used in the fusion. The pearls were then taken to an induction oven to obtain disk-shaped samples with approximately 37 mm in diameter and 5 mm of thickness, which were used in the analyses. The minimum thickness required depends on the grain size range of the sample, and a small grain size is required to yield chemical homogeneity without absorption problems when applying XRF.

The quantitative analyses were performed using SemiQ software, and five scans were carried out to detect all the elements present in the sample (except for H, C, Li, Be, B, N, O, and the transuranic elements). Additionally, both materials were also subject to observation (conducted at 5,000× magnification) in a scanning electron microscope (FESEM), JEOL JSM 6700F (JEOL, Tokyo) with an acceleration voltage of 20 kV in high vacuum at a working distance of approximately of 15 mm. The micrographs were taken with a backscattered electron detector (BSE). A description of these tests has been given by Rondón-Quintana et al. (2019).

Based on XRF, the main chemical compounds of PF [Fig. 1(a)] and NF [Fig. 1(b)] are given in Table 2. The chemical composition of the PF is similar to that reported by the manufacturer (Fosfatos del Huila 2022). Mineral compounds of both fillers are provided in Table 3. These mineral contents are similar to those reported by Calle (2016) and Rojas (2022).

Images of the SEM observations are shown in Fig. 2. In general terms, PF particles have a rougher texture. The smoother surface texture of NF could be due to its high SiO_2 content. The elemental composition of the NF and PF particles obtained through SEM is provided in Table 4.

Aggregate and asphalt binder [asphalt cement AC 60/70, 0.1-mm penetration range according to ASTM D5 (ASTM 2013); performance grade PG 64-22] properties are given in Tables 5 and 6, respectively. Both materials were characterized following the INVIAS (2022) standard. The tests performed on the AC 60/70 were penetration (ASTM D5), penetration index [NLT-181 (NLT 1988)], softening point [ASTM D36 (ASTM 2006)], viscosity [ASTM D4402 (ASTM 2015)], flash and fire points [ASTM D3143 (ASTM 2019)], ductility [ASTM D113 (ASTM 1999)], and the rolling thin-film oven test [ASTM D2872-12e1 (ASTM 2012)].

The tests performed on the natural aggregate were specific gravity and absorption [AASHTO T 84 (AASHTO 2000) and AASHTO T 85 (AASHTO 1991)], fractured particles [ASTM D5821 (AASHTO 2001)], soundness of aggregate using magnesium sulfate [AASHTO T 104 (AASHTO 1999)], plasticity index [ASTM D4318 (ASTM 2000)], 10% fines [DNER-ME 096 (DNER 1998)], Micro-Deval [AASHTO T327 (AASHTO 2005)], and Los Angeles machine [AASHTO T 96 (AASHTO 2002)]. Properties of both materials met INVIAS (2022) requirements and specifications for the manufacture of HMAs in Colombia.

Asphalt Mastic Properties

Asphalt mastics were manufactured with both fillers (NF and PF) using a filler/asphalt binder ratio of 1.2. The binder and fillers

(a) (b)

Fig. 1. (a) PF; and (b) NF.

Table 2. Chemical composition of NF and PF

XRF results			
	Composition (%)		PF (Fosfatos del Huila 2022)
Element	NF	PF	
Phosphorous (P_2O_5)	0.1	32.2	28.0
Calcio (CaO)	1.6	39.1	38.0
Silica (SiO_2)	61.9	11.6	14.0
Fluorine (F)	—	2.5	3.0
Carbon (C)	—	1.7	1.0
Aluminum (Al_2O_3)	10.8	1.2	0.5
Iron (Fe_2O_3)	5.6	0.2	0.4
Sulfur (SO_4)	—	0.1	0.3
Magnesium (MgO)	3.0	0.1	0.1
Sodium (Na_2O)	2.2	—	0.1
Potassium (K_2O)	1.2	—	0.1
Titanium (TiO_2)	1.0	—	—

Table 3. Mineral percentages in the PF and NF samples (XRD test)

Sample	Mineral	Chemical formula	Percentage by mass
PF	Fluorapatite	$Ca_5(PO_4)_3F$	56.6
	Calcite	$CaCO_3$	22.5
	Quartz	SiO_2	20.8
NF	Quartz	SiO_2	61.0
	Albite	$Na(AlSi_3O_8)$	25.1
	Illite	$(K, H_3O)(Al, Mg, Fe)_2(Si, Al)_4O_{10}$	5.3
	Chlorite	$(Mg, Fe)_3(Si, Al)_4O_{10}$; $(OH)_2 \cdot (Mg, Fe)_3(OH)_6$	8.7

(NF and PF) blend were performed at 120°C by using a high-shear mixing machine at a speed of 3,000 revolutions per minute (rpm) for 20 min. Higher temperatures and longer mixing times were not used in order not to age the mastic. Penetration tests (ASTM 2013) were performed at four temperatures (10°C, 20°C, 30°C, and 40°C), and softening point (ASTM 2006), ductility (ASTM 1999), and rotational viscosity (RV) (ASTM 2015) tests were also carried out. Penetration and RV tests results are shown in Figs. 3 and 4, respectively. Softening point and ductility test results are given in Table 7.

It is observable that PF asphalt mastic displayed greater stiffness (less penetration and ductility, and greater softening point and viscosity) in comparison with NF. This greater stiffness can be due to the high fluorapatite and quartz content present in PF (both add up to more than 78% of the mineralogical composition). Fluorapatite is a bioactive, biocompatible mineral that displays an antibacterial behavior, as well as high stability and hardness (because of this reason, it is widely used in bone repair) (Seyedmajidi and Seyedmajidi 2022). Likewise, quartz could develop high strength and interlocking in the mineral skeleton and is a material with high levels of hardness and mechanical strength (Muniandy et al. 2013; Rondón-Quintana et al. 2018). Additionally, the amount of P_2O_5 could increase this stiffness, as occurs in asphalt mixtures modified with PPA (Liu et al. 2018).

Using a dynamic shear rheometer (DSR) [AASHTO T 315 (AASHTO 2020)], the complex shear modulus (G^*) and phase angle (δ) of NF and PF asphalt mastics were measured under strain-controlled mode (strain level was 1% and frequency range was 1–100 rad/s). The test temperatures were 35°C and 64°C. Samples of 8-mm diameter and a DSR parallel plate with a 2-mm gap were tested at 35°C. For the case of 64°C, these dimensions were 25 mm in diameter and 1-mm gap. Five duplicate specimens were tested for each individual asphalt mastic, and the average value was reported. $G^*/\sin\delta$ results are shown in Fig. 5.

G^* is related to the strength and overall stiffness of asphalt mastics (Cheng et al. 2016; Bastidas-Martínez et al. 2021), and this parameter increased with the rise of frequency. Using PF as filler resulted in increased stiffness of asphalt mastic compared with

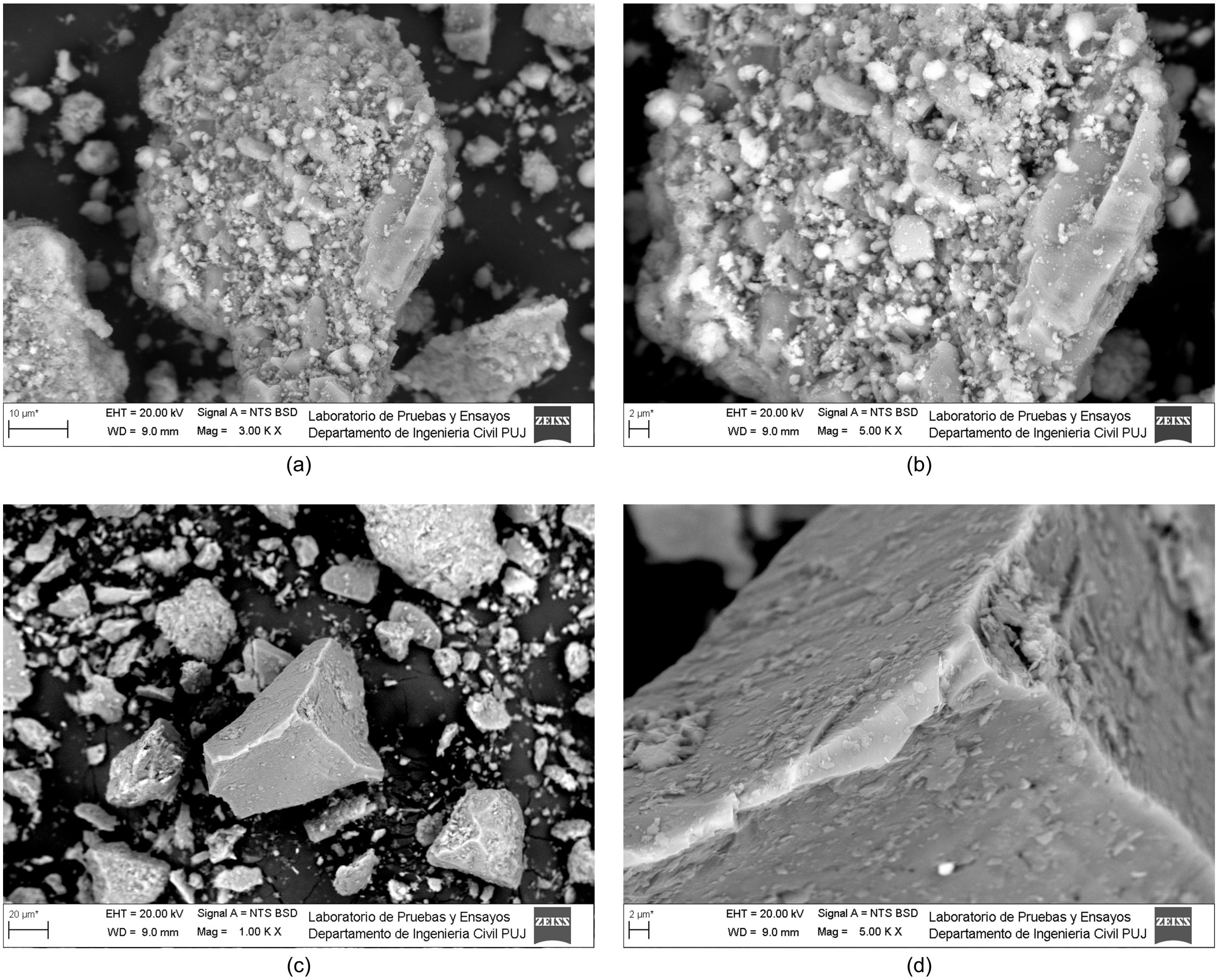

Fig. 2. SEM observations: (a) PF at 3,000×; (b) PF at 5,000×; (c) NF at 1,000×; and (d) NF at 5,000×.

Table 4. Elemental composition of NF and PF particles based on SEM

	Element (%)											
Particle type	C	O	Ca	P	Si	Al	Cu	Fe	Na	Mg	K	Ti
NF	31.4	45.5	0.1	0.0	15.6	3.5	0.1	1.1	0.1	0.3	1.3	0.2
PF	31.3	39.8	16.8	6.1	3.5	0.6	0.2	0.2	0.1	0.1	0.0	0.0

Table 5. Aggregate properties

Test	Method	Recommended	Result
Specific gravity/fine aggregate absorption	AASHTO T 84	—	2.62/1.5%
Specific gravity/coarse aggregate absorption	AASHTO T 85	—	2.56/1.6%
Fractured particles (1 side)	ASTM D5821	85% minimum	90.5%
Soundness of aggregate using magnesium sulfate	AASHTO T 104	18.0% maximum	6.5%
Plasticity index	ASTM D4318	Not plastic	Not plastic
10% of fines (dry resistance)	DNER-ME 096	100 kN minimum	134.9 kN
Micro-Deval	AASHTO T 327	20% maximum	17.8%
Abrasion in Los Angeles machine	AASHTO T 96	25% maximum	21.6%

Table 6. AC 60/70 properties

Test	Method	Unit	Recommended	Result
		Tests on the original asphalt		
Specific gravity	AASHTO T 228	—	—	1.018
Penetration (25°C, 100 g, 5 s)	ASTM D5	0.1 mm	60–70	63.2
Penetration Index	NLT 181	—	−1.2/+0.6	−0.78
Viscosity (60°C)	AASHTO T 316	Poise	1,500 minimum	1,806
Softening point	ASTM D36	°C	48–54	49.5
Ductility (25°C, 5 cm/min)	ASTM D113	cm	100 minimum	>105
Flash and fire points	ASTM D5821	°C	230 minimum	291
		Tests on the residue after rolling thin-film oven test		
Mass loss	ASTM D2872	%	0.8 maximum	0.51
Penetration (25°C, 100 g, 5 s)	ASTM D5	%	50 minimum	79.4

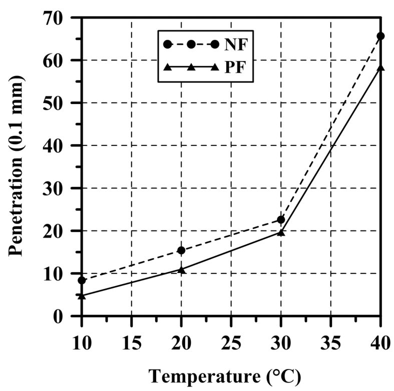

Fig. 3. Penetration of asphalt mastics.

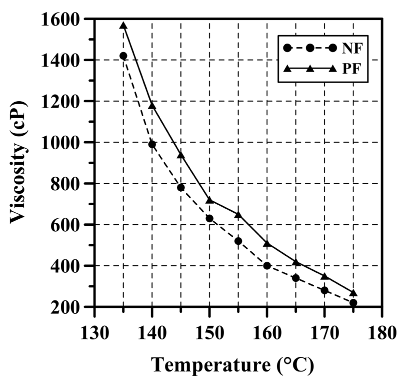

Fig. 4. Viscosity curve of asphalt mastics.

NF. The results are consistent with those of conventional asphalt characterization tests (penetration, ductility, and softening point) and RV. PF asphalt mastic showed greater resistance to rutting and better performance at high temperature of service compared with NF asphalt mastic.

Hot-Mix Asphalt Manufacture and Design

Two types of HMA samples were manufactured for the tests: control HMA (comprised entirely of NF) and HMA-PF (NF filler replaced by PF). Particle-size distributions of HMA mixtures are given in Table 8 (total filler 6%). The maximum HMA particle size was 19 mm. Tests were carried out on Marshall type samples [AASHTO T 245 (AASHTO 2015)] with diameter and height of 101.6 and 63.5 mm, respectively). Mix and compaction temperatures were 150°C and 145°C, respectively (obtained based on the viscosity curve of AC 60/70). In order to compact the samples, these were subjected to 75 blows per face.

Table 7. Softening point and ductility of NF and PF

Mastic	Softening point (°C)	Ductility (cm)
NF	51.8	32.5
PF	52.6	29.5

Asphalt mix design was carried out following the criteria established by INVIAS (2022) and through performing Marshall tests [AASHTO T 245 (AASHTO 2015)]. In order to obtain optimum asphalt binder content (OAC), five samples were manufactured for each asphalt binder content of 4.5%, 5.0%, 5.5%, and 6.0% (in relation to HMA mass). In total, 20 samples were manufactured for control HMA and 20 for HMA-PF. Stability (S), flow (F), and S/F ratio parameters were measured using a Marshall apparatus. Monotonic load was applied at a rate of 50.8 mm per minute on samples at 60°C. Additionally, volumetric parameters were calculated [air void content (Va), voids in the mineral aggregate (VMA), and voids filled with asphalt (VFA)].

Indirect Tensile Strength Test

The ITS [AASHTO T 283 (AASHTO 2018)] was performed on samples manufactured with the OAC and volumetric composition obtained from the Marshall mix design procedure. Using a Marshall compression machine, monotonic load was applied radially at 50.8 mm/min on three dry samples (ITS-D) for each HMA mix (control and HMA-PF) at 25°C. Three other conditioned samples for each HMA mix were tested at 25°C after conditioning for 24 h submerged in water at 60°C (ITS-C). Moisture damage resistance was evaluated using TSR as a percentage through the ITS-C/ITS-D ratio.

Resilient Modulus, Permanent Deformation, and Fatigue Resistance

Tests under cyclic load were carried out in a Nottingham Asphalt Tester (NAT). Resilient modulus (RM) was obtained using an indirect tensile half-sine load type under frequencies of 2.5, 5.0, and 10 Hz and temperatures of 20°C, 30°C, and 40°C (all specimens were conditioned for 4 h at each temperature prior to testing). The UNE-EN 12697-26 (UNE-EN 2019c) procedure was followed. Each RM was determined based on the average of results obtained on three cylindrical Marshall samples. In order to measure RM,

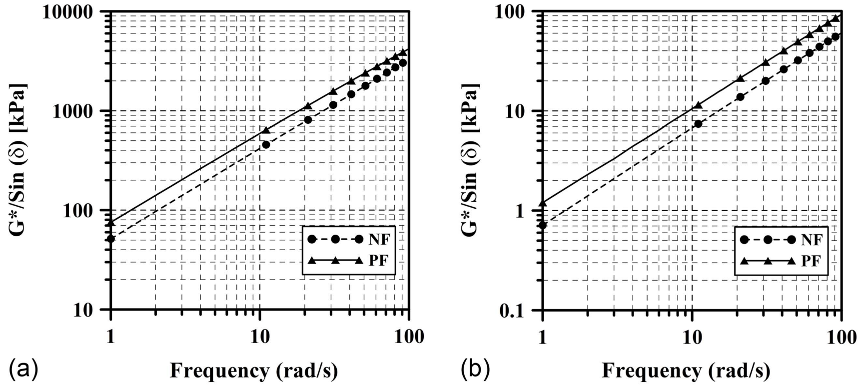

Fig. 5. Evolution of $G^*/\sin(\delta)$ with load frequency for (a) 35°C; and (b) 64°C.

a Poisson ratio of 0.35 was assumed. Load amplitude was controlled to maintain a deformation level lower than 50 microstrains.

The UNE-EN 12697-25 (UNE-EN 2019b) specification was followed for permanent deformation resistance tests. Accumulation of permanent deformation was measured on samples at 40°C. Load cycles were square wave type with a frequency of 0.5 Hz (1 s of load application and 1 s of rest per cycle). In total, 600 cycles of preload (10 kPa) were applied for 20 min, then 3,600 load cycles under a stress of 100 kPa were applied. Vertical displacement in each cycle was measured using LVDTs. Permanent deformation curves were established by averaging the results obtained on three Marshall samples.

The UNE-EN 12697-24 (UNE-EN 2019a) specification was followed for indirect tensile fatigue resistance tests. The fatigue tests were conducted in controlled-stress mode. Test temperature was 20°C. Load frequency was 10 Hz. Total rupture of the sample was the failure criterion chosen to obtain the number of cycles to failure (N_f). Nine Marshall samples were used to obtain each fatigue curve (three samples for each stress levels of 250, 350, and 450 kPa).

Cantabro Test

This test was carried out to determine the abrasion loss of compacted HMAs specimens following the Tex-245-F (TxDOT 2021) specification. A Los Angeles abrasion machine was used (without steel spheres). Test temperature was room temperature (20°C). Weight loss percentage [Cantabro loss (CL)] was estimated through a relationship between mass lost in the test after applying 500 cycles and the sample's initial mass. CL was calculated by averaging the results of three Marshall samples.

Results

Marshall Test

Marshall test results are given in Table 9 and shown in Fig. 6. Considering INVIAS (2022) design specifications criteria, OAC was 5%. Mixes that used PF as filler displayed greater resistance under monotonic load (greater S and S/F). In regards to OAC, the HMA-PF mix displayed an increase of 12.3% and 35.1% in S and S/F, respectively, in comparison with the control mix. Based on the ANOVA analysis ($F > F_{0.05}$), resistance changes were statistically significant. A greater S/F is considered to be an indirect indicator of rutting resistance in high-temperature climates. This greater resistance was achieved despite the Va of the HMA-PF mix being slightly greater. This greater Va was obtained as a product of a greater difficulty for mixing the aggregate and the asphalt, as the mastic stiffens.

Table 8. HMA particle size distribution

Sieve	Passing (%)
3/4 in.	100
1/2 in.	87.5
3/8 in.	79.0
No. 4	57.0
No. 10	37.0
No. 40	19.5
No. 80	12.5
No. 200	6.0

Indirect Tensile Strength Test-ITS

ITS test results are presented in Fig. 7. A greater ITS can be observed in mixes that used PF (ITS-D and ITS-C increased by an average of 17.3%). This greater ITS was statistically significant based on ANOVA analysis ($F > F_{0.05}$). Despite the aforementioned findings, moisture damage resistance evaluated through the TSR parameter was similar (96.5% for the NF mix and 96.6% for the PF mix). In general, materials with a greater CaO/SiO_2 ratio displayed a stronger bond with asphalt binders (Xie et al. 2012), and the interfacial energy and adhesion work of the asphalt components with mineral aggregates were greater (Guo et al. 2016). This could explain the greater ITS obtained in the HMA-PF mix ($CaO/SiO_2 = 0.026$ and 2.71 for NF and PF, respectively). Additionally, the PF mastic was stiffer in comparison with the NF mastic.

Cantabro Tests

This test is widely used in porous asphalt mix design. In dense mixes, it can be used in order to provide durability indexes, including for non-load-associated cracking, raveling, and weathering (Cox et al. 2017). According to Doyle and Howard (2016), the Cantabro test could be recommended for consideration as a durability index for dense-graded asphalt mixtures. Cantabro test results are given in Table 10. A greater Cantabro resistance can be observed when the mix that used PF was subjected to this test. This greater resistance was statistically significant based on ANOVA analysis ($F > F_{0.05}$).

Resilient Modulus and Permanent Deformation

Resilient modulus test results are shown in Fig. 8. The typical behavior of the resilient modulus was observed: it increased with

J. Mater. Civ. Eng., 2023, 35(9): 04023274

Table 9. Marshall test results

AC (%)	S (kN)	F (mm)	S/F (kN/mm)	Va (%)	VMA (%)	VFA (%)
			Control			
4.5	13.68 ± 0.09	3.89 ± 0.07	3.51 ± 0.09	5.98 ± 0.47	16.03 ± 0.42	62.75 ± 1.98
5.0	15.53 ± 0.26	3.77 ± 0.06	4.12 ± 0.02	3.61 ± 0.07	14.98 ± 0.06	75.90 ± 0.36
5.5	14.78 ± 0.14	4.02 ± 0.08	3.68 ± 0.10	2.26 ± 0.25	14.86 ± 0.22	84.77 ± 1.43
6.0	14.43 ± 0.13	4.28 ± 0.10	3.38 ± 0.04	1.24 ± 0.16	15.02 ± 0.14	91.78 ± 1.00
			HMA-PF			
4.5	14.77 ± 0.34	3.43 ± 0.13	4.31 ± 0.20	6.77 ± 0.11	16.76 ± 0.10	59.60 ± 0.42
5.0	17.45 ± 0.34	3.13 ± 0.07	5.57 ± 0.06	4.71 ± 0.07	15.97 ± 0.07	70.53 ± 0.34
5.5	16.31 ± 0.16	3.18 ± 0.12	5.14 ± 0.16	4.14 ± 0.29	16.51 ± 0.25	74.96 ± 1.39
6.0	15.56 ± 0.29	3.85 ± 0.06	4.04 ± 0.11	2.01 ± 0.21	15.71 ± 0.18	87.20 ± 1.21

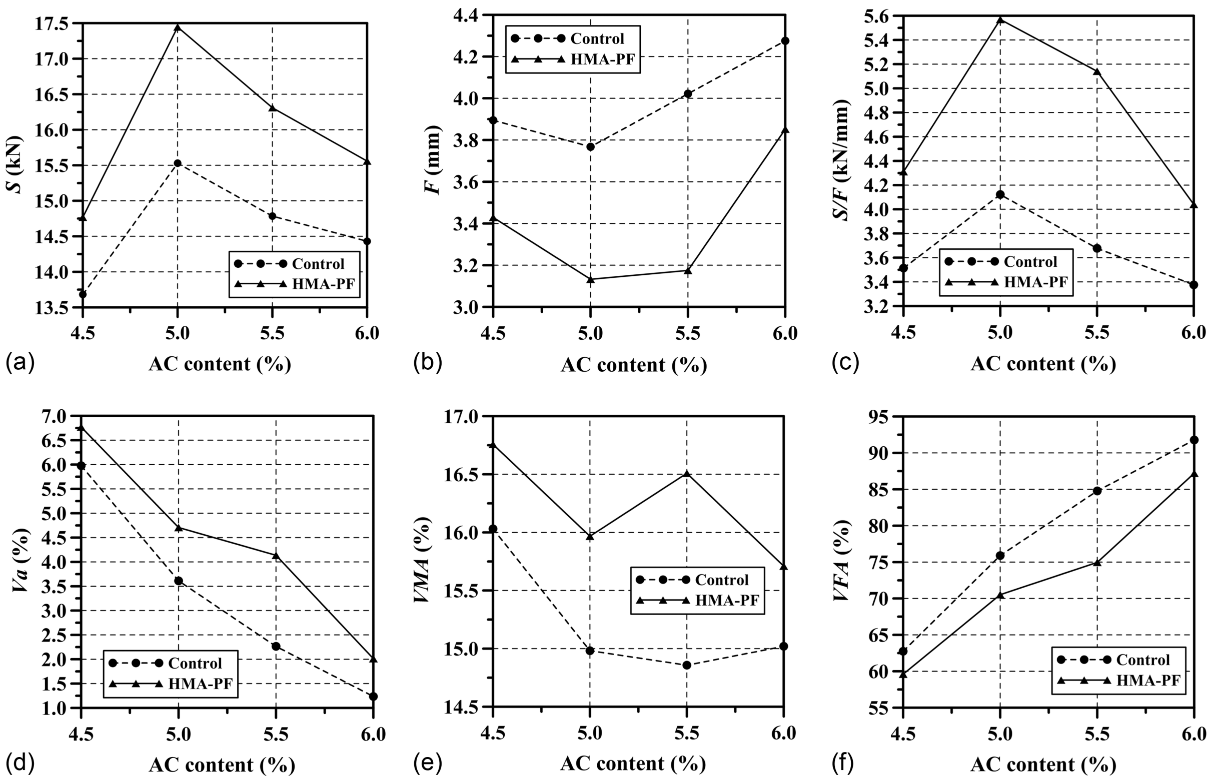

Fig. 6. Evolution of (a) S; (b) F; (c) S/F ratio; (d) Va content; (e) VMA; and (f) VFA with AC content.

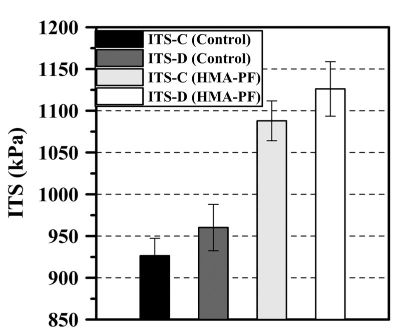

Fig. 7. ITS test results.

Table 10. Cantabro test results

Mixture	Va (%)	Mass loss CL (%) at 500 revolutions
Control	4.1	8.8 ± 0.37
HMA-PF	4.4	7.2 ± 0.26

the increase of loading frequency and decreased with the increase of test temperature. A statistically significant increase could be observed (ANOVA; $F > F_{0.05}$) in resilient modulus when mixes used PF. These results are coherent with the greater S and S/F ratio obtained in the Marshall test and the greater stiffness in the mastic that used PF. As previously described in the properties of the asphalt mastic, the P_2O_5 content and the mineralogical composition of the PF could influence the increase in resilient modulus. The greater stiffness of the HMA-PF mix under cyclic load caused an increase in permanent deformation resistance (Fig. 9).

Fatigue Resistance

Fatigue test results are shown in Fig. 10. A greater resistance can be observed when the mix used PF. Fatigue law slopes (b) are similar ($b = -0.202$ and -0.208 for control mix and HMA-PF mix, respectively). However, σ_6 (stress magnitude for $N_f = 10^6$) is of 196.4 and 208.4 kPa for the control mix and HMA-PF mix, respectively. The increase of fatigue resistance can be due to the greater resistance obtained in HMA-PF in ITS tests (Teltayev and Radovskiy 2018).

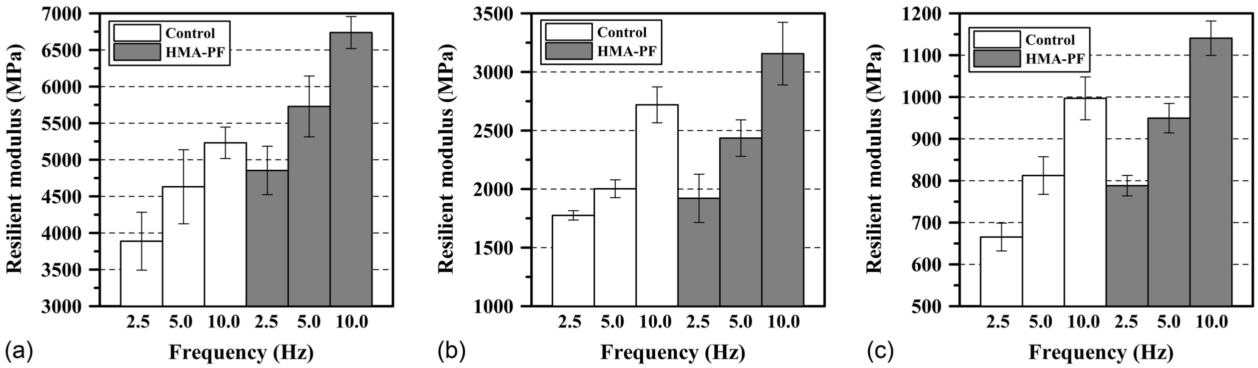

Fig. 8. Resilient modulus test results at (a) 20°C; (b) 30°C; and (c) 40°C.

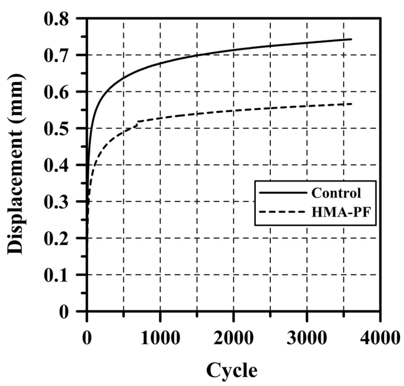

Fig. 9. Permanent deformation test results.

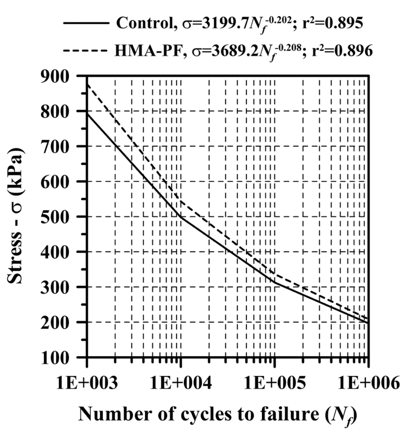

Fig. 10. Fatigue test results.

The CaO/SiO_2 ratio was higher in the PF, improving aspects associated with the cohesion and adhesion of the asphalt mix. The rougher texture of PF particles could improve asphalt binder-aggregate adhesion. In addition, under controlled stress, fatigue resistance tends to increase when mix stiffness increases (Elseifi et al. 2003; Di Benedetto et al. 2004; Muniz de Farias et al. 2018; Ruiz-Ibarra et al. 2020; Bharath et al. 2021; Bastidas-Martínez et al. 2022). This loading mode (controlled stress) better simulates the fatigue response of mixtures that make up thick asphalt layers (Elseifi et al. 2003; Rondón-Quintana et al. 2021).

Conclusions

This study replaced a natural-origin filler in a hot-mix asphalt with phosphorite. Based on the results obtained, conclusions are the following:

- Phosphorite maintains the optimum asphalt binder content and helps to increase hot-mix asphalt resistance (1) under monotonic load in the Marshall test, (2) under indirect tension, (3) to rutting (increase in permanent deformation resistance and resilient modulus), and (4) to fatigue under controlled-stress.
- Regarding moisture damage resistance, the TSR parameter was similar in mixes with natural filler and phosphorite; however, ITS-C and ITS-D were superior in mixes with phosphorite.
- Phosphorite could help to improve the performance of a hot-mix asphalt in high-temperature climates and in thick asphalt layers in pavements.

It is important to highlight that the results are valid for the type of mix, aggregate, asphalt binder, phosphate rock, and analysis conditions used in the foregoing study. This study must be seen as the first phase in a research line. Future studies must (1) use other types of aggregates, fillers and phosphate rocks, asphalt binders, gradations, and analysis temperatures, among others; (2) measure and evaluate physical-chemical and rheological interactions of phosphorite with asphalt binders; (3) evaluate aging and low-temperature cracking resistance; and (4) conduct an economic and environmental analysis.

Data Availability Statement

Some or all data, models, or code generated or used during the study are available from the corresponding author by request.

Acknowledgments

We thank the participating institutions (Universidad Distrital Francisco José de Caldas, Pontificia Universidad Javeriana, Universidad Militar Nueva Granada, and Universidad Piloto de Colombia) for the support granted to researchers.

References

AASHTO. 1991. *Standard method of test for specific gravity and absorption of coarse aggregate*. AASHTO T 85. Washington, DC: AASHTO.

AASHTO. 1999. *Standard method of test for soundness of aggregate by use of sodium sulfate or magnesium sulfate*. AASHTO T 104. Washington, DC: AASHTO.

AASHTO. 2000. *Standard method of test for specific gravity and absorption of fine aggregate*. AASHTO T 84. Washington, DC: AASHTO.

AASHTO. 2002. *Standard method of test for resistance to degradation of small-size coarse aggregate by abrasion and impact in the Los Angeles machine*. AASHTO T 96. Washington, DC: AASHTO.

AASHTO. 2005. *Standard method of test for resistance of coarse aggregate to degradation by abrasion in the micro-deval apparatus*. AASHTO T 327. Washington, DC: AASHTO.

AASHTO. 2015. *Standard method of test for resistance to plastic flow of bituminous mixtures using Marshall apparatus*. AASHTO T 245. Washington, DC: AASHTO.

AASHTO. 2018. *Standard method of test for resistance of compacted asphalt mixtures to moisture-induced damage*. AASHTO TP 283-14. Washington, DC: AASHTO.

AASHTO. 2019. *Standard method of test for density of hydraulic cement*. AASHTO T 133. Washington, DC: AASHTO.

AASHTO. 2020. *Standard method of test for determining the rheological properties of asphalt binder using a ynamic shear rheometer (DSR)*. AASHTO T 315. Washington, DC: AASHTO.

Aflaki, S., and N. Tabatabaee. 2009. "Proposals for modification of Iranian bitumen to meet the climatic requirements of Iran." *Constr. Build. Mater.* 23 (6): 2141–2150. https://doi.org/10.1016/j.conbuildmat.2008.12.014.

ASTM. 1999. *Standard test method for ductility of bituminous materials*. ASTM D113. West Conshohocken, PA: ASTM.

ASTM. 2000. *Standard test methods for liquid limit, plastic limit, and plasticity index of soils*. ASTM D4318. West Conshohocken, PA: ASTM.

ASTM. 2001. *Standard test method for determining the percentage of fractured particles in coarse aggregate*. ASTM D5821. West Conshohocken, PA: ASTM.

ASTM. 2006. *Standard test method for softening point of bitumen (ring and- ball apparatus)*. ASTM D36. West Conshohocken, PA: ASTM.

ASTM. 2012. *Standard test method for effect of heat and air on a moving film of asphalt (rolling thin-film oven test)*. ASTM D2872-12e1. West Conshohocken, PA: ASTM.

ASTM. 2013. *Standard test method for penetration of bituminous materials*. ASTM D5/D5M. West Conshohocken, PA: ASTM.

ASTM. 2015. *Standard test method for viscosity determination of asphalt at elevated temperatures using a rotational viscometer*. ASTM D4402/D4402M. West Conshohocken, PA: ASTM.

ASTM. 2019. *Standard test method for flash point of cutback asphalt with tag open-cup apparatus*. ASTM D3143. West Conshohocken, PA: ASTM.

Bastidas-Martínez, J. G., J. Camapum de Carvalho, L. L. Cristhiane, M. Muniz de Farias, and H. A. Rondón-Quintana. 2022. "Effects of iron ore tailing on performance of hot-mix asphalt." *J. Mater. Civ. Eng.* 34 (1): 04021405 https://doi.org/10.1061/(ASCE)MT.1943-5533.0004034.

Bastidas-Martínez, J. G., H. A. Rondón-Quintana, and M. Muniz de Farias. 2021. "Behavior of asphalt mastics containing different materials as filler." *Can. J. Civ. Eng.* 48 (4): 347–355. https://doi.org/10.1139/cjce-2019-0342.

Bharath, G., K. S. Reddy, V. Tandon, and M. A. Reddy. 2021. "Aggregate gradation effect on the fatigue performance of recycled asphalt mixtures." *Road Mater. Pavement Des.* 22 (1): 165–184. https://doi.org/10.1080/14680629.2019.1620116.

Calle, S. M. 2016. *Evaluación de la acidulación de roca fosfórica empleando la bacteria acidófila Acidithiobacillus thiooxidans*. Medellín: Universidad Nacional de Colombia.

Cheng, Y., J. Tao, Y. Jiao, G. Tan, Q. Guo, S. Wang, and P. Ni. 2016. "Influence of the properties of filler on high and medium temperature performances of asphalt mastic." *Constr. Build. Mater.* 118 (Aug): 268–275. https://doi.org/10.1016/j.conbuildmat.2016.05.041.

Cox, B. C., B. T. Smith, I. L. Howard, and R. S. James. 2017. "State of knowledge for Cantabro testing of dense graded asphalt." *J. Mater. Civ. Eng.* 29 (10): 04017174 https://doi.org/10.1061/(ASCE)MT.1943-5533.0002020.

Cuadri, A. A., F. J. Navarro, M. García-Moralesa, and J. P. Bolívar. 2014. "Valorization of phosphogypsum waste as asphaltic bitumen modifier." *J. Hazard. Mater.* 279 (Aug): 11–16. https://doi.org/10.1016/j.jhazmat.2014.06.058.

Cuadri, A. A., S. Pérez-Moreno, C. L. Altamar, F. J. Navarro, and J. P. Bolívar. 2021. "Phosphogypsum as additive for foamed bitumen manufacturing used in asphalt paving." *J. Cleaner Prod.* 283 (Feb): 124661. https://doi.org/10.1016/j.jclepro.2020.124661.

Di Benedetto, H., C. De La Roche, H. Baaj, A. Pronk, and R. Lundström. 2004. "Fatigue of bituminous mixtures." *Mater. Struct. Constr.* 37 (3): 202–216. https://doi.org/10.1007/BF02481620.

DNER (Departamento Nacional de Estradas de Rodagem). 1998. *Avaliação da resistência mecânica pelo método dos 10% de finos [Evaluation of mechanical resistance to coarse aggregate using 10% method]*. DNER-ME 096. Rio de Janeiro, Brazil: Departamento Nacional de Infraestrutura de Transporte.

Doyle, J. D., and I. L. Howard. 2016. "Characterization of dense-graded asphalt with the Cantabro test." *J. Test. Eval.* 44 (1): 77–88. https://doi.org/10.1520/JTE20140212.

Elseifi, M. A., G. W. Flintsch, and I. L. Al-Qadi. 2003. "Quantitative effect of elastomeric modification on binder performance at intermediate and high temperatures." *J. Mater. Civ. Eng.* 15 (1): 32–40. https://doi.org/10.1061/(ASCE)0899-1561(2003)15:1(32).

Fosfatos del Huila. 2022. "Ficha Técnica de 'Fosforita 28P'." Accessed March 20, 2022. http://fosfatosdelhuila.com/fhportal/descargas/FICHA%20TECNICA%20FOSFORITA%2028P%20V.3%20-%20copia.pdf.

Foxworthy, P. T., R. S. Nadimpalli, and R. K. Seals. 1996. "Phosphogypsum slag aggregate-based asphaltic concrete mixes." *J. Transp. Eng.* 122 (4): 300–307. https://doi.org/10.1061/(ASCE)0733-947X(1996)122:4(300).

Ge, D., K. Yan, L. You, and Z. Wang. 2017. "Modification mechanism of asphalt modified with Sasobit and Polyphosphoric acid (PPA)." *Constr. Build. Mater.* 143 (Jul): 419–428. https://doi.org/10.1016/j.conbuildmat.2017.03.043.

Ghabchi, R., S. Rani, M. Zaman, and S. A. Ali. 2021. "Effect of WMA additive on properties of PPA-modified asphalt binders containing anti-stripping agent." *Int. J. Pavement Eng.* 22 (4): 418–431. https://doi.org/10.1080/10298436.2019.1614584.

Guo, M., Y. Tan, A. Bhasin, J. Wei, X. Yang, and Y. Hou. 2016. "Using molecular dynamics to investigate interfacial adhesion between asphalt binder and mineral aggregate." In *Proc., 4th Chinese-European Workshop on Functional Pavement Design (4th CEW 2016)*, edited by S. Erkens, X. Liu, K. Anupam, and Y. Tan, 517–527. Delft, Netherlands: Taylor & Francis Group.

Hajikarimi, P., F. F. Tehrani, F. M. Nejad, J. Absi, M. Rahi, A. Khodaii, and C. Petit. 2018. "Generalized fractional viscoelastic modeling of low temperature characteristics of asphalt binders modified with polyphosphoric acid and distillate aromatic extracts oil." *J. Mater. Civ. Eng.* 30 (7): 04018147 https://doi.org/10.1061/(ASCE)MT.1943-5533.0002353.

Hao, P., R. Zhai, Z. Zhang, and X. Cao. 2019. "Investigation on performance of polyphosphoric acid (PPA)/SBR compound-modified asphalt mixture at high and low temperatures." *Road Mater. Pavement Des.* 20 (6): 1376–1390. https://doi.org/10.1080/14680629.2018.1447503.

Hossain, Z., M. S. Alam, and G. Baumgardner. 2020. "Evaluation of rheological performance and moisture susceptibility of polyphosphoric acid modified asphalt binders." *Road Mater. Pavement Des.* 21 (1): 237–252. https://doi.org/10.1080/14680629.2018.1483261.

Huang, S., F. P. Miknis, W. Schuster, S. Salmans, M. Farrar, and R. Boysen. 2011. "Rheological and chemical properties of hydrated lime and polyphosphoric acid–modified asphalts with long-term aging." *J. Mater. Civ. Eng.* 23 (5): 628–637. https://doi.org/10.1061/(ASCE)MT.1943-5533.0000219.

INVIAS (Instituto Nacional de Vías). 2022. *Especificaciones generales de construcción de carreteras*. Bogotá, DC, Colombia: INVIAS.

Jafari, M., and A. Babazadeh. 2016. "Evaluation of polyphosphoric acid-modified binders using multiple stress creep and recovery and linear amplitude sweep tests." *Road Mater. Pavement Des.* 17 (4): 859–876. https://doi.org/10.1080/14680629.2015.1132631.

Jafari, M., A. A. Nasrekani, M. Nakhaei, and A. Babazadeh. 2017. "Evaluation of rutting resistance of asphalt binders and asphalt mixtures modified with polyphosphoric acid." *Pet. Sci. Technol.* 35 (2): 141–147. https://doi.org/10.1080/10916466.2016.1248776.

Jiang, X., P. Li, Z. Ding, L. Yang, and J. Zhao. 2019. "Investigations on viscosity and flow behavior of polyphosphoric acid (PPA) modified asphalt at high temperatures." *Constr. Build. Mater.* 228 (Dec): 116610. https://doi.org/10.1016/j.conbuildmat.2019.07.336.

Katamine, N. M. 2000. "Phosphate waste in mixtures to improve their deformation." *J. Transp. Eng.* 126 (5): 382–389. https://doi.org/10.1061/(ASCE)0733-947X(2000)126:5(382).

Liang, P., M. Liang, W. Fan, Y. Zhang, C. Qian, and S. Ren. 2017. "Improving thermo-rheological behavior and compatibility of SBR modified asphalt by addition of polyphosphoric acid (PPA)." *Constr. Build. Mater.* 139 (May): 183–192. https://doi.org/10.1016/j.conbuildmat.2017.02.065.

Liu, H., M. Zhang, Y. Wang, Z. Chen, and P. Hao. 2020. "Rheological properties and modification mechanism of polyphosphoric acid-modified asphalt." *Road Mater. Pavement Des.* 21 (4): 1078–1095. https://doi.org/10.1080/14680629.2018.1537931.

Liu, J., K. Yan, and J. Liu. 2018. "Rheological characteristics of polyphosphoric acid–modified asphalt mastic." *J. Mater. Civ. Eng.* 30 (12): 06018021 https://doi.org/10.1061/(ASCE)MT.1943-5533.0002555.

Liu, J., K. Yan, L. You, D. Ge, and Z. Wang. 2016. "Laboratory performance of warm mix asphalt binder containing polyphosphoric acid." *Constr. Build. Mater.* 106 (Mar): 218–227. https://doi.org/10.1016/j.conbuildmat.2015.12.126.

Ma, F., C. Li, Z. Fu, Y. Huang, J. Dai, and Q. Feng. 2021. "Evaluation of high temperature rheological performance of polyphosphoric acid-SBS and polyphosphoric acid-crumb rubber modified asphalt." *Constr. Build. Mater.* 306 (Nov): 124926. https://doi.org/10.1016/j.conbuildmat.2021.124926.

Maghsoodloorad, H., H. Khalili, and A. Allahverdi. 2018. "Alkali-activated phosphorous slag performance under different curing conditions: Compressive strength, hydration products, and microstructure." *J. Mater. Civ. Eng.* 30 (1): 04017253 https://doi.org/10.1061/(ASCE)MT.1943-5533.0002101.

Masson, J.-F. 2008. "Brief review of the chemistry of polyphosphoric acid (PPA) and bitumen." *Energy Fuels* 22 (4): 2637–2640. https://doi.org/10.1021/ef800120x.

Miknis, F. P., and K. P. Thomas. 2008. "NMR Analysis of polyphosphoric acid-modified bitumens." *Road Mater. Pavement Des.* 9 (1): 59–72. https://doi.org/10.1080/14680629.2008.9690107.

Muniandy, R., E. Aburkaba, and R. Taha. 2013. "Effect of mineral filler type and particle size on the engineering properties of stone mastic asphalt pavements." *J. Eng. Res.* 10 (2): 13–32. https://doi.org/10.24200/tjer.vol10iss2pp13-32.

Muniz de Farias, M., F. Qui˜nonez-Sinisterra, and H. A. Rondón-Quintana. 2018. "Behavior of a hot-mix asphalt made with recycled concrete aggregate and crumb rubber." *Can. J. Civ. Eng.* 70 (Apr): 1–39. https://doi.org/10.1139/cjce-2018-0443.

NLT (Normas del Laboratorio de Transporte). 1988. *Método para determinar la variacion de la consistencia del betún asfáltico con los cambios de temperatura (susceptibilidad) [Method to determine the variation in the consistency of asphalt bitumen with temperatura changes (susceptibility)]*. Norma NLT-181. Madrid, Spain: NLT.

Orange, G., J. V. Martin, A. Menapace, M. Hemsley, and G. L. Baumgardner. 2004. "Rutting and moisture resistance of asphalt mixtures containing polymer and polyphosphoric acid modified bitumen." *Road Mater. Pavement Des.* 5 (3): 323–354. https://doi.org/10.1080/14680629.2004.9689975.

Pasandín, A. R., and I. Pérez. 2015. "The influence of the mineral filler on the adhesion between aggregates and bitumen." *Int. J. Adhes. Adhes.* 58 (Apr): 53–58. https://doi.org/10.1016/j.ijadhadh.2015.01.005.

Qian, C., W. Fan, F. Ren, X. Lv, and B. Xing. 2019a. "Influence of polyphosphoric acid (PPA) on properties of crumb rubber (CR) modified asphalt." *Constr. Build. Mater.* 227 (Dec): 117094. https://doi.org/10.1016/j.conbuildmat.2019.117094.

Qian, G., S. Bai, S. Ju, and T. Huang. 2013. "Laboratory evaluation on recycling waste phosphorus slag as the mineral filler in hot-mix asphalt." *J. Mater. Civ. Eng.* 25 (7): 846–850. https://doi.org/10.1061/(ASCE)MT.1943-5533.0000770.

Qian, G., K. Wang, X. Bai, T. Xiao, D. Jin, and Q. Huang. 2018. "Effects of surface modified phosphate slag powder on performance of asphalt and asphalt mixture." *Constr. Build. Mater.* 158 (Apr): 1081–1089. https://doi.org/10.1016/j.conbuildmat.2017.09.123.

Qian, G., H. Yu, X. Gong, and W. Zheng. 2019b. "Effect of phosphorus slag powder on flammability properties of asphalt." *J. Mater. Civ. Eng.* 31 (11): 04019280 https://doi.org/10.1061/(ASCE)MT.1943-5533.0002951.

Rojas, P. A. 2022. *Identificación de cadmio (Cd) soluble en rocas fosfóricas y su relación con diversas propiedades encontradas sobre yacimientos empleados para la producción de fertilizantes de la Cordillera Oriental*. Medellín, Colombia: Trabajo de grado, Geología, Departamento de Ciencias de la Tierra, Universidad EAFIT.

Rondón-Quintana, H. A., F. A. Reyes-Lizcano, and C. A. Zafra-Mejía. 2021. "Fatigue in asphalt mixtures—A summary to understand the complexity of its mathematical modeling." *J. Phys. Conf. Ser.* 2118 (1): 012009. https://doi.org/10.1088/1742-6596/2118/1/012009.

Rondón-Quintana, H. A., J. C. Ruge-Cárdenas, J. G. Bastidas-Martínez, M. Y. Velandia-Castelblanco, and M. Muniz de Farias. 2020. "Use of thermally treated bentonite as filler in hot mix asphalt." *J. Mater. Civ. Eng.* 32 (5): 04020070 https://doi.org/10.1061/(ASCE)MT.1943-5533.0003127.

Rondón-Quintana, H. A., J. C. Ruge-Cárdenas, and M. Muniz de Farias. 2019. "Behavior of hot-mix asphalt containing blast furnace slag as aggregate: Evaluation by mass and volume substitution." *J. Mater. Civ. Eng.* 31 (2): 04018364 https://doi.org/10.1061/(ASCE)MT.1943-5533.0002574.

Rondón-Quintana, H. A., J. C. Ruge-Cárdenas, D. F. Patiño-Sánchez, H. A. Vacca-Gamez, F. A. Reyes-Lizcano, and M. Muniz de Farias. 2018. "Blast furnace slag as a substitute for the fine fraction of aggregates in an asphalt mixture." *J. Mater. Civ. Eng.* 30 (10): 04018244 https://doi.org/10.1061/(ASCE)MT.1943-5533.0002409.

Ruiz-Ibarra, J. F., H. A. Rondón-Quintana, and S. Chavez-Pabón. 2020. "Behavior of a warm mix asphalt containing a blast furnace slag." *Int. J. Civ. Eng.* 18: 325–334. https://doi.org/10.1007/s40999-019-00475-6.

Seyedmajidi, S., and M. Seyedmajidi. 2022. "Fluorapatite: A review of synthesis, properties and medical applications vs hydroxyapatite." *Iran. J. Mater. Sci. Eng.* 19 (2): 1–20. https://doi.org/10.22068/ijmse.2430.

Sheng, Y., B. Zhang, Y. Yan, H. Chen, R. Xiong, and J. Geng. 2017. "Effects of phosphorus slag powder and polyester fiber on performance characteristics of asphalt binders and resultant mixtures." *Constr. Build. Mater.* 141 (Jun): 289–295. https://doi.org/10.1016/j.conbuildmat.2017.02.141.

Sobhi, S., A. Yousefi, and A. Behnood. 2020. "The effects of Gilsonite and Sasobit on the mechanical properties and durability of asphalt mixtures." *Constr. Build. Mater.* 238 (Mar): 117676. https://doi.org/10.1016/j.conbuildmat.2019.117676.

Song, R., A. Sha, K. Shi, J. Li, X. Li, and F. Zhang. 2021. "Polyphosphoric acid and plasticizer modified asphalt: Rheological properties and modification mechanism." *Constr. Build. Mater.* 309 (Nov): 125158. https://doi.org/10.1016/j.conbuildmat.2021.125158.

Teltayev, B., and B. Radovskiy. 2018. "Predicting thermal cracking of asphalt pavements from bitumen and mix properties." *Road Mater. Pavement Des.* 19 (8): 1832–1847. https://doi.org/10.1080/14680629.2017.1350598.

TxDOT. 2021. *Test Procedure for Cantabro loss*. Tex-245-F. Austin, TX: Dept. of Transportation.

UNE-EN. 2019a. *Bituminous mixtures—Test methods—Part 24: Resistance to fatigue*. UNE-EN 12697-24:2019. Madrid, Spain: 1NLT.

UNE-EN. 2019b. *Bituminous mixtures—Test methods—Part 25: Cyclic compression test*. UNE-EN 12697-25:2019. Madrid, Spain: 1NLT.

UNE-EN. 2019c. *Bituminous mixtures—Test methods—Part 26: Stiffness*. UNE-EN 12697-26:2019. Madrid, Spain: 1NLT.

Xie, J., S. Wu, J. Lin, J. Cai, Z. Chen, and W. Wei. 2012. "Recycling of basic oxygen furnace slag in asphalt mixture: Material characterization & moisture damage investigation." *Constr. Build. Mater.* 36 (Nov): 467–474. https://doi.org/10.1016/j.conbuildmat.2012.06.023.

Yu, H., S. Li, G. Qian, X. Gong, and K. Wang. 2020a. "Experiment evaluation on the surface treatment of phosphorus slag (PS) micropowder for asphalt modification." *Constr. Build. Mater.* 262 (Nov): 119931. https://doi.org/10.1016/j.conbuildmat.2020.119931.

Yu, H., X. Zhu, G. Qian, X. Gong, and X. Nie. 2020b. "Evaluation of phosphorus slag (PS) content and particle size on the performance modification effect of asphalt." *Constr. Build. Mater.* 256 (Sep): 119334. https://doi.org/10.1016/j.conbuildmat.2020.119334.

Ziari, M. A., P. Hajikarimi, A. K. Kazerooni, F. M. Nejad, and E. H. Fini. 2021. "Effect of polyphosphoric acid on fracture properties of asphalt binder and asphalt mixtures." *Constr. Build. Mater.* 310 (Dec): 125240. https://doi.org/10.1016/j.conbuildmat.2021.125240.